Custom-designed arrays of anodic alumina nanochannels with individually tunable pore sizes

2014 Nanotechnology 25 335301

(http://iopscience.iop.org/0957-4484/25/33/335301)

IOP Publishing Nanotechnology
Nanotechnology **25** (2014) 335301 (5pp) doi:10.1088/0957-4484/25/33/335301

Custom-designed arrays of anodic alumina nanochannels with individually tunable pore sizes

Kun-Tong Tsai[1,2], Chih-Yi Liu[3,4], Huai-Hsien Wang[2], Ting-Yu Liu[5], Ming-Yu Lai[2], Jr-Hau He[1] and Yuh-Lin Wang[2,6]

[1] Institute of Photonics and Optoelectronics and Department of Electrical Engineering, National Taiwan University, Taipei 10617, Taiwan
[2] Institute of Atomic and Molecular Sciences, Academia Sinica, PO Box 23-166, Taipei 10617, Taiwan
[3] Department of Electrical Engineering, National Cheng Kung University, Tainan 70101, Taiwan
[4] Advanced Optoelectronic Technology Center, National Cheng Kung University, Tainan 70101, Taiwan
[5] Department of Materials Engineering, Ming Chi University of Technology, New Taipei City 24301, Taiwan
[6] Department of Physics, National Taiwan University, Taipei 10617, Taiwan

E-mail: jhhe@cc.ee.ntu.edu.tw and ylwang@pub.iams.sinica.edu.tw

Received 9 April 2014, revised 16 June 2014
Accepted for publication 24 June 2014
Published 25 July 2014

Abstract

We demonstrate a process to selectively tune the pore size of an individual nanochannel in an array of high-aspect-ratio anodic aluminum oxide (AAO) nanochannels in which the pore sizes were originally uniform. This novel process enables us to fabricate arrays of AAO nanochannels of variable sizes arranged in any custom-designed geometry. The process is based on our ability to selectively close an individual nanochannel in an array by using focused ion beam (FIB) sputtering, which leads to redeposition of the sputtered material and closure of the nanochannel with a capping layer of a thickness depending on the energy of the FIB. When such a partially capped array is etched in acid, the capping layers are dissolved after different time delays due to their different thicknesses, which results in differences in the time required for the following pore-widening etching processes and therefore creates an array of nanochannels with variable pore sizes. The ability to fabricate such AAO templates with high-aspect-ratio nanochannels of tunable sizes arranged in a custom-designed geometry paves the way for the creation of nanophotonic and nanoelectronic devices.

S Online supplementary data available from stacks.iop.org/NANO/25/335301/mmedia

Keywords: focused ion beam, lithography, anodic aluminum oxide, high-aspect-ratio nanochannel, tunable pore size, template-assisted synthesis

(Some figures may appear in colour only in the online journal)

1. Introduction

Porous anodic aluminum oxide (AAO) templates with arrays of self-organized nanochannels that have extremely uniform pore sizes and channel lengths and channel aspect ratios that can easily reach as high as $100 \sim 1000$ have been widely used as templates for the synthesis of nanocomposites [1–17] and as masks or stamps for nanolithography and device fabrications [1–6] for use in a variety of applications ranging from photovoltaics [4, 6], photonic crystal [7], biosensing [8–10], nanophotonics, and nanodevices [5, 11] to metamaterials [9, 12–19]. Such high-aspect-ratio nanochannel arrays are unique and inaccessible by conventional lithographic methods, making them promising as templates for the construction of metamaterial with controllable nanocomposite over the entire structure. For example, AAO templates have

been used to grow arrays of parallel silver nanowires via electrochemical deposition, creating metamaterial with negative refraction [12, 16]. These templates have also been used to grow metamaterial slab lenses for focusing visible light [14] and superlenses for use in high-resolution imaging [19].

To further broaden the applications of AAO templates for the fabrication of nanocomposites with more stringent precision in their physical properties, many attempts have been made to control the initial position and pore configuration of the nanochannels formed on AAO templates as a means of enriching the variety of pattern configurations. In this effort, lithographic guiding methods have been used; these includenanoimprint lithography [20, 21], three-beam interference lithography [22], focued ion beam (FIB) lithography [23–26], and template molding [27]. Pulse anodization has also been used [28, 29]. Nanochannel arrays with square lattices [20, 30], triagular lattices [20], moiré patterns [31, 32], and modulation of pore diameters along the pore axes [28, 29] have been fabricated, and pore geometries with square [20, 30], triangular [20] and other shapes [33] as well as gradient diameters [26] have also been achieved. However, it is notable that only nanochannel arrays with hexagonally close-packed (HCP) lattices are likely to reach an aspect ratio of larger than 10 without channel branching or termination. The intrinsic dendritic nature of an isolated AAO nanochannel [20, 26, 34] is more likely to be effectively suppressed by the precise confinement from its surrounding nanochannels arranged in an HCP lattice.

Such AAO templates with HCP lattices can be made even more flexible for the design and construction of sophisticated nanocomposites with local variation in their physical properties. These new kinds of AAO template could be made if the diameter of an individual nanochannel in an array could be selectively controlled and if nanochannels of different sizes could be arranged in a custom-designed configuration. Such a fabrication process would greatly enhance the potential to use porous AAO templates as technological platforms for the creation of nanophotonic devices and metamaterials.

Here, we demonstrate a two-step process capable of forming complex configurations comprising nanochannels with tunable pore sizes as well as maintaining their high-aspect-ratio architectures in arrays of AAO nanochannels. In this process, FIB lithography is employed to selectively create a capping layer of desired thickness on an individual nanochannel. The capping layer is then used to delay the start of the pore-widening etching process when the entire array is subsequently immersed in an etchant. Capping layers of different thicknesses create different delays in the start of the etching processes and therefore create nanochannels of different pore sizes at the end of the process.

The development of this unique combination of FIB lithography and selective pore-widening of individual nanochannels in an array constitutes an important step towards broadening the applications of AAO templates in the creation of nanocomposites and metamaterials.

2. Experimental details

High-purity aluminum substrate was first polished in a mixture of 50% $HClO_4$ and C_2H_5OH (1:5 v v^{-1}). A 50 keV FIB system was then used to create an array of HCP lattice in a concave shape on the substrate to initial the growth of nanochannels with an 'ideally-matched' [35] lattice of 100 nm having an HCP arrangement during anodization by 0.3 M oxalic acid at a constant voltage of 40 V. The pore-widening process was carried out by immersing the sample in a 6 wt% H_3PO_4 solution at 38 °C. The pore size of ~46 nm on the nanochannel arrays was set to be the initial condition (uncapped substrate) in all cases for the experimental demonstrations of creating the AAO nanochannels arrays with various pore sizes.

Closure of the nanochannels was carried out and monitored *in situ* in a 30 keV dual beam FIB system (FEI, NOVA 600). More details about the fabrication of the capping layers can be found elsewhere [24, 25] and in figure S1 (as shown in schematics of supplementary figures S1(a)–(c) and in the transmission electron microscope image of the capped nanochannel arrays of supplementary figure S1(d) available at stacks.iop.org/NANO/25/335301/mmedia).

3. Results and discussion

Figure 1 depicts schematically the two-step process we used to create an array of high-aspect-ratio nanochannels with different pore sizes on AAO templates. First, a thin capping layer that delays the etching on the side wall of the nanochannels formed spontaneously on top of the nanochannels on the AAO templates in response to FIB sputtering (figures 1(a), (b)). Second, the capping layers delayed chemical etching on the side wall of the nanochannels and resulted in nanochannels of different pore sizes on the AAO template, as shown in figures 1(b), (c).

To demonstrate the feasibility of delayed chemical etching, the nanochannels were selectively closed (in the right regions) and kept opened (in the left regions) as shown in the scanning electron microscopy (SEM) image in figure 1(d) (corresponding to the schematic in figure 1(b)). We closed the nanochannels by covering them with a thin capping layer created by using FIB irradiation with a beam energy of 20 keV and a dose of 5×10^{16} ion cm^{-2}. Immersing the samples in an etchant of H_3PO_4 for 15 min yielded arrays of nanochannels with two different pore sizes, as shown in figure 1(e) (corresponding to the schematic in figure 1(c)). The side walls of nanochannels without a capping layer were directly etched, leading to nanochannels of larger diameter, whereas the etching process for nanochannels with a capping layer was delayed until the capping layer was etched. Therefore, nanochannels with different pore sizes were obtained; the pore sizes of the nanochannels with and without delayed chemical etching were ~50 nm and ~80 nm, respectively.

This result verifies that the nanochannel pore size is tunable via the delayed chemical etching process by using a

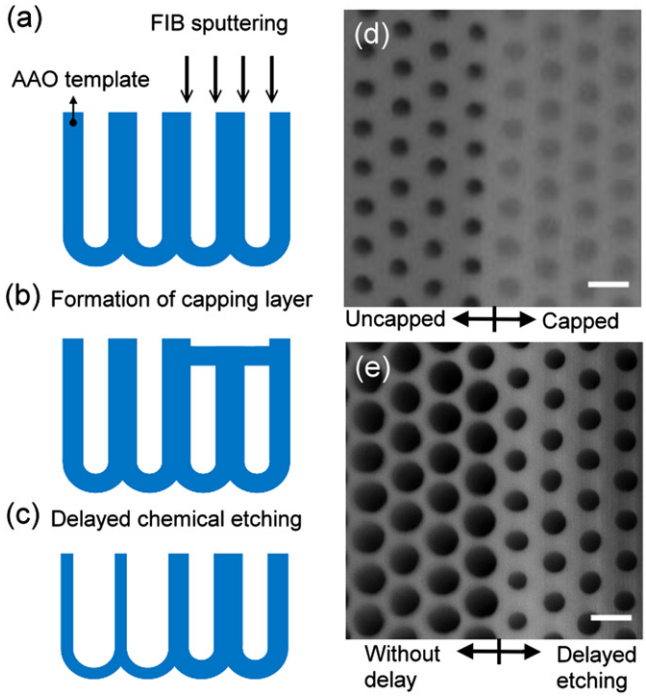

Figure 1. Schematics of fabrication processes (a)–(c) and experimental demonstration using FIB induced channel closing and delayed chemical etching (d), (e) to create nanochannels with different pore sizes on AAO templates. (a) FIB sputtering for selectively closing nanochannels, (b) selective formation of thick capping layer after ion irradiation, (c) chemical etching for removing/thinning capping layer and thus forming nanochannels with different pore sizes, (d) SEM images of nanochannel arrays on AAO templates with and without thin capping layer at right and left regions, respectively, and (e) SEM images of nanochannels with different pore sizes after chemical etching. Scale bars in (d) and (e) are 100 nm.

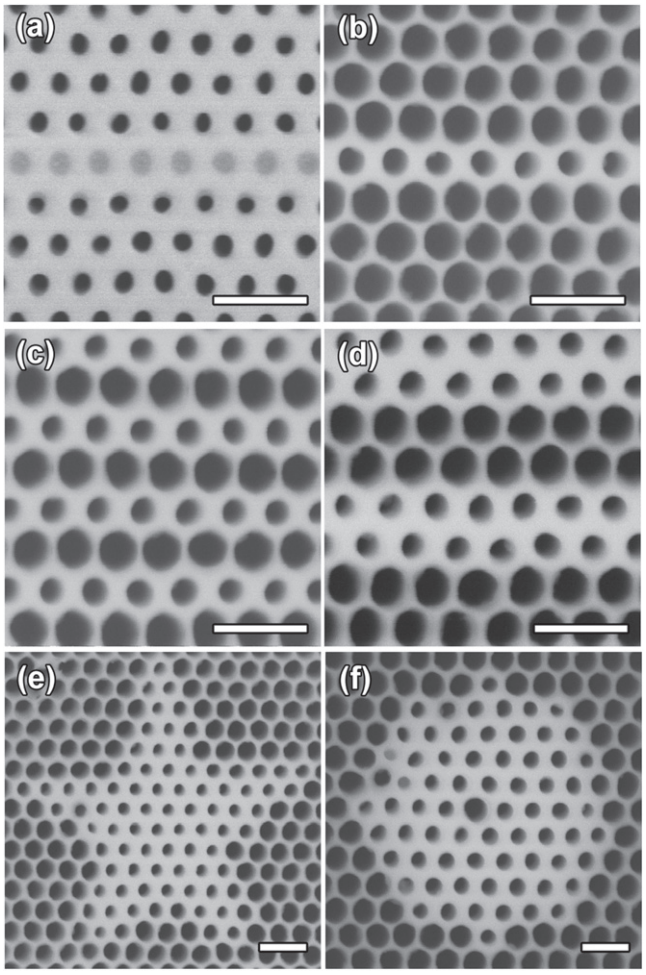

Figure 2. SEM images of (a) closed nanochannels arranged in a single line, and nanochannels with two different pore sizes arranged in (b) a single line, (c) single line arrays, (d) double line arrays, (e) star, and (f) a hexagonal array with a nanochannel of larger pore size at its center (scale bars are 200 nm).

capping layer as a protecting layer. The result also shows that the pore size of nanochannels remains uniform after etching, which indicates that the present technique is promising for the design of nanoscale device arrays.

Since our proposed process is readily able to create nanochannels with different pore sizes, we took another significant step towards the creation of the patterns used to construct nanodevices by focusing on spatial resolution of the lithography. To determine the usefulness of this technique, we used a 20 keV Ga ion beam with a dose of 5×10^{16} ion cm^{-2} to create patterns of closed nanochannel arrays on the AAO templates, as shown in figure 2(a). The SEM image of nanochannel arrays reopened after the etching is shown in figure 2(b).

These results show the possibility of having an individually addressable resolution on both closing and reopening the nanochannel, which is unprecedented. Repeating the patterns creates a line array (grating-like), as shown in figure 2(c). Nanochannels arranged in more complicated geometries such as double-line arrays and star-shape arrays can also be fabricated (figures 2(d) and (e)). Figure 2(f) shows a single nanochannel with large pore sizes surrounded by nanochannels with small diameters (i.e., introduction of a defect) arranged in a hexagonal geometry (photonic crystal-like). We are investigating whether we can fill the nanochannels with metals to serve as a plasmonic waveguide [36] that will confine the light in this nanostructure.

The success of the delayed chemical etching process hinges on the capping layer's serving as a self-organized masking layer that is extremely uniform and therefore can be etched uniformly even at the single-pore level. The mechanism of forming a thin capping layer is associated with dynamic equilibrium between the materials that are sputtered away from the surface and the replenishment either from re-deposition of material ejected from the side wall of the nanochannels or from ion-induced material migration. Accordingly, the thickness of the capping layer is determined primarily by beam energy and an applied dose of FIB irradiation [24, 25]. When an AAO nanochannel is irradiated by higher-energy ions, more materials are replenished and a thicker capping layer is formed. By using this interesting mechanism for forming the self-organized capping layer, it is possible to fabricate capping layers of different thicknesses that result in different delays in the subsequent pore-widening process.

Figure 3 shows the pore size as a function of etching time for nanochannels covered by capping layers created by using

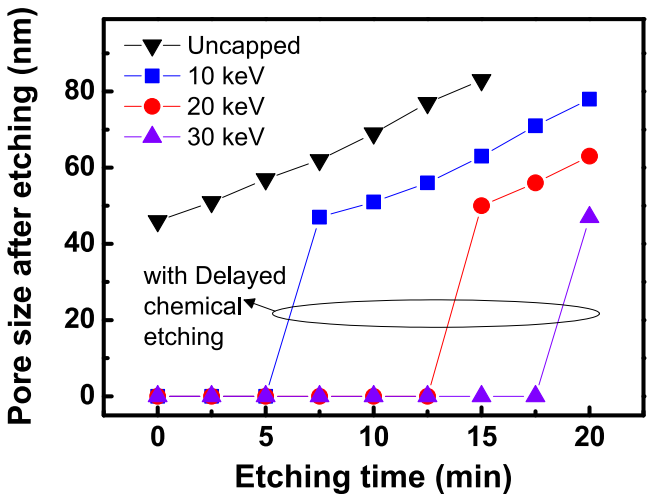

Figure 3. Pore size as a function of etching time for nanochannels covered by capping layers created by FIB of different energies.

FIB of different energies. The figure clearly shows our ability to precisely control the thickness of the capping layer and therefore the delay in the subsequent pore-widening process. For example, the time required for removing the capping layers created at beam energies of 10 keV, 20 keV, and 30 keV are 7.5 min, 15 min, and 20 min 30 keV, respectively. Notably, capping layers created by different beam energies are etched at similar rates, which implies that the chemical composition and microstructure of the capping layers created within a variety of ion-beam energy ranges are almost identical. In addition, the rates at which the capping layer and the side wall of an AAO nanochannel are etched is on the same order of ~1 nm min^{-1}. Therefore, pores of different sizes can be readily tuned by simply varying the beam energy of the FIB employed to form the capping layer.

The process just described enables us to lithographically define the patterns on selective areas by using different beam energies to construct the arrays of nanochannels with multiple pore sizes on AAO templates, as shown by the schematics illustrated in figure 4(a). For example, figures 4(b) and (c) show SEM images of an AAO nanochannel array before and after its different areas have been exposed to FIB of different energies (15 keV to 30 keV respectively). After immersion in the H_3PO_4 for 17.5 min, the pores are fully (partially) opened on the patterned area defined by beam energies of 15 keV and 20 keV (25 keV) as shown in figure 4(d), clearly demonstrating the differences in the pore sizes. At longer etching times, all the pores are opened and pore sizes ranging from 48 nm to 80 nm are created. The ability to fabricate high-aspect-ratio nanochannels of certain pore sizes in a specific area makes possible many applications such as creaton of flat sub-micron graded-index lenses and templates filled with metallic nanowires for the creation of metallic microlenses [37], which are very challenging to fabricate owing to the necessary high aspect ratio of the nanowires.

Instead of using several beam energies to fabricate a capping layer with the desired thickness, an alternative method is to form a thicker layer by using the higher energy beam first and then reducing the thickness of the capping layer by using a relatively low beam energy with different doses (as shown in the schematics of supplementary figures S2(a)–(d) available at stacks.iop.org/NANO/25/335301/mmedia). This approach has the advantage of controling the thickness of the capping layer simply by changing the dose of the lower energy beam. Here, the high beam energy (30 kV, for example) was first used to

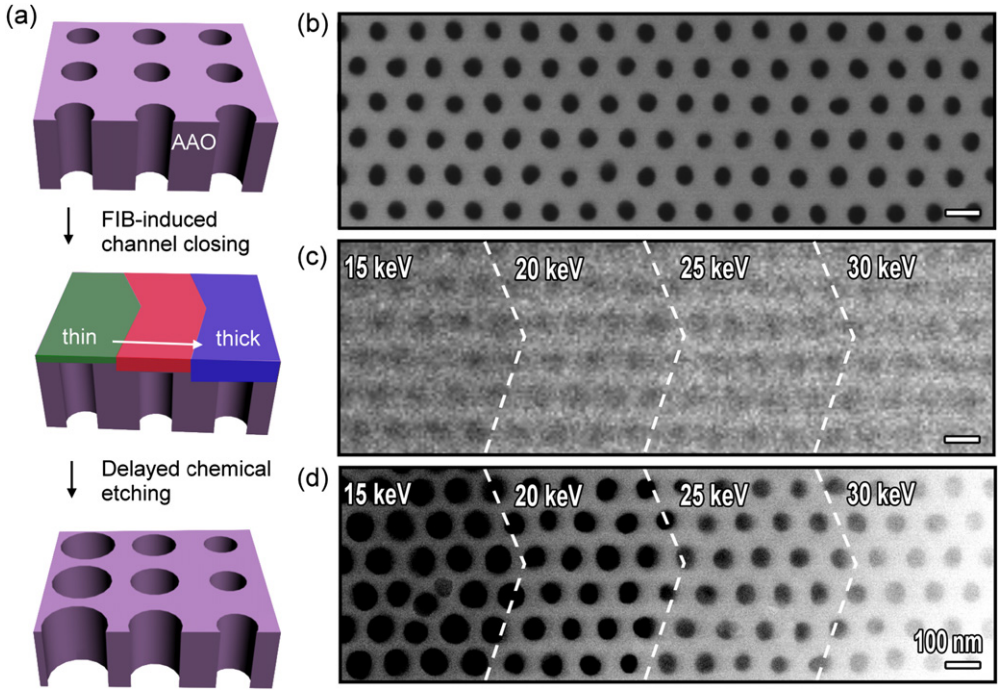

Figure 4. (a) Schematics showing the fabrication process to create the AAO template with nanochannels of different pore sizes. (b) and (c) SEM images of an ordered array of AAO nanochannels before and after being covered by capping layers created by FIB of different energies. (d) Nanochannel arrays with graded pore sizes created after etching (scale bars are 100 nm).

form a capping layer of ~30 nm thickness; then low-beam energy (10 kV, for example) was used to reduce the thickness of the capping layer. The duration of the etching time and the corresponding pore sizes are summarized in figure S3 (see the supplementary data available at stacks.iop.org/NANO/25/335301/mmedia). The area that received more doses is thinner and the pores are reopened first. Both approaches provide exciting opportunities to create meso/macroporous AAO templates with tunable pore sizes, which are otherwise difficult to fabricate by conventional lithography techniques.

4. Conclusion

In summary, we have developed a process to create arrays of high-aspect-ratio AAO nanochannels with tunable pore sizes. Pore size differences of 5–40 nm are readily created by using capping layers with different thicknesses formed by FIB sputtering. Using the process to provide spatial resolution down to the single-pore level is feasible, which indicates that the technique shows promise as a means of creating the patterns needed for nanodevice applications. Such templates are very hard to fabricate by conventional lithographical techniques, and the methods used here offer a new way to provide meso/macroporous materials with designable pore size (porosity) arranged in any custom-designed geometry. Our process can be easily applied to customize AAO templates with high-aspect-ratio nanochannels, the channel diameters of which are very hard to change selectively with other lithographical techniques. This unique combination of FIB lithography and delayed chemical etching of AAO nanochannel arrays facilitates the fabrication of templates needed for constructing novel nanophotonic devices, such as plasmonic waveguides and metallic lenses.

Acknowledgements

This work has been supported by National Science Council of Taiwan (NSC 101-2120-M-001-001-CC1, NSC 102-2628-M-001-008). Technical support from the Core Facilities for Nanoscience and Nanoctechnology at Academia Sinica, Taiwan, are acknowledged. KTT acknowledges support from National Science Council of Taiwan via the Graduate Student Study Abroad Program of Taiwan.

References

[1] Wang H S, Chen S Y, Su M H, Wang Y L and Wei K-H 2010 *Nanotechnology* **21** 203505
[2] Wang H S, Lin L H, Chen S Y, Wang Y L and Wei K-H 2009 *Nanotechnology* **20** 075201
[3] Yamada N, Ijiro T, Okamoto E, Hayashi K and Masuda H 2011 *Opt. Express* **19** A118–25
[4] Chang C Y, Wu C E, Chen S Y, Cui C H, Cheng Y J, Hsu C S, Wang Y L and Li Y F 2011 *Angew. Chem. Int. Ed.* **50** 9386–90
[5] Son J Y, Shin Y H, Kim H and Jang H M 2010 *ACS Nano* **4** 2655–8
[6] Wang H P, Tsai K T, Lai K Y, Wei T C, Wang Y L and He J H 2012 *Opt. Express* **20** A94–103
[7] Choi J, Luo Y, Wehrspohn R B, Hillebrand R, Schilling J and Gösele U 2003 *J. Appl. Phys.* **94** 4757–62
[8] Liu T Y, Tsai K T, Wang H H, Chen Y, Chen Y H, Chao Y C, Chang H H, Lin C H, Wang J K and Wang Y L 2011 *Nat. Commun.* **2** 538
[9] Kabashin A V, Evans P R, Pastkovsky S, Hendren H, Wurtz G A, Atkinson R, Pollard R J, Podolskiy V A and Zayats A V 2009 *Nat. Mater.* **8** 867–71
[10] McPhillips J, Murphy A, Jonsson M P, Hendren W R, Atkinson R, Hook F, Zayats A V and Pollard R J 2010 *ACS Nano* **4** 2210–6
[11] Herderick E D, Reddy K M, Sample R N, Draskovic T I and Padture N P 2009 *Appl. Phys. Lett.* **95** 203505
[12] Yao J, Liu Z W, Liu Y M, Wang Y, Sun C, Bartal G, Stacy A M and Zhang X 2008 *Science* **321** 930
[13] Pollard R J, Murphy A, Hendren W R, Evans P R, Atkinson R, Wurtz G A, Zayats A V and Podolskiy V A 2009 *Phys. Rev. Lett.* **102** 127405
[14] Yao J, Tsai K T, Wang Y, Liu Z, Bartal G, Wang Y L and Zhang X 2009 *Opt. Express* **17** 22380–5
[15] Tsai K T, Huang Y R, Lai M Y, Lu C Y, Wang H H, He J H and Wang Y L 2010 *J. Nanosci. Nanotechnol.* **10** 8293–7
[16] Noginov M A, Barnakov Y A, Zhu G, Tumkur T, Li H and Narimanov E E 2009 *Appl. Phys. Lett.* **94** 151105
[17] Alekseyev L V, Narimanov E E, Tumkur T, Li H, Barnakov Y A and Noginov M A 2010 *Appl. Phys. Lett.* **97** 131107
[18] Yao J, Wang Y, Tsai K T, Liu Z, Yin X, Bartal G, Stacy A M, Wang Y L and Zhang X 2011 *Phil. Trans. R. Soc.* A **369** 3434–46
[19] Casse B D F, Lu W T, Huang Y J, Gultepe E, Menon L and Sridhar S 2010 *Appl. Phys. Lett.* **96** 023114
[20] Masuda H, Asoh H, Watanabe M, Nishio K, Nakao M and Tamamura T 2001 *Adv. Mater.* **13** 189–92
[21] Kustandi T S, Loh W W, Gao H and Low H Y 2010 *ACS Nano* **4** 2561–8
[22] de Boor J, Geyer N, Göesele U and Schmidt V 2009 *Opt. Lett.* **34** 1783–5
[23] Liu C Y, Datta A and Wang Y L 2001 *Appl. Phys. Lett.* **78** 120–2
[24] Liu N W, Datta A, Liu C Y, Peng C Y, Wang H H and Wang Y L 2005 *Adv. Mater.* **17** 222–5
[25] Liu N W, Liu C Y, Wang H H, Hsu C F, Lai M Y, Chuang T H and Wang Y L 2008 *Adv. Mater.* **20** 2547–51
[26] Chen B, Lu K and Tian Z 2010 *Electrochim. Acta* **56** 435–40
[27] Biring S, Tsai K T, Sur U K and Wang Y L 2008 *Nanotechnology* **19** 015304
[28] Lee W, Schwirn K, Steinhart M, Pippel E, Scholz R and Göesele U 2008 *Nat. Nanotechnol.* **3** 234–9
[29] Lee W and Kim J-C 2010 *Nanotechnology* **21** 485304
[30] Asoh H, Ono S, Hirose T, Takatori I and Masuda H 2004 *Jap. J. Appl. Phys.* **43** 6342–6
[31] Choi J, Wehrspohn R B and Gösele U 2005 *Electrochim. Acta* **50** 2591–5
[32] Chen B and Lu K 2011 *Langmuir* **27** 4117–25
[33] Liu C Y, Lai M Y, Tsai K T, Chang H H, He J H, Shiue J and Wang Y L 2013 *Nanotechnology* **24** 055306
[34] Chen S Y, Chang H H, Lai M Y, Liu C Y and Wang Y L 2011 *Nanotechnology* **22** 365303
[35] Liu C Y, Datta A, Liu N W, Peng C Y and Wang Y L 2004 *Appl. Phys. Lett.* **84** 2509–11
[36] Schmidt M A, Prill Sempere L N, Tyagi H K, Poulton C G and Russell P S J 2008 *Phys. Rev.* B **77** 033417
[37] Verslegers L, Catrysse P B, Yu Z F, Shin W, Ruan Z C and Fan S H 2010 *Opt. Lett.* **35** 844–6